Composites Communications 20 (2020) 100357

Contents lists available at ScienceDirect

Composites Communications

journal homepage: www.elsevier.com/locate/coco

Functionalized water molecules confined in hydrogels for energy mitigation by assembling liquid nanofoams in micro polymeric pockets

Chi Zhan, Mingzhe Li, Weiyi Lu *

Department of Civil and Environmental Engineering, Michigan State University, East Lansing, MI, 48824, USA

ARTICLE INFO

Keywords:
Hydrogel
Liquid nanofoam
Hydrophobic nanoporous particles
Energy mitigation

ABSTRACT

In this work, we report the development of an innovative energy dissipative hydrogel. The hydrogel is constructed by assembling liquid nanofoam, composed of hydrophobic nanoporous particles and water molecules, into the polyacrylamide (PAM)-based hydrogel network. Under the hydrostatic loading condition, water molecules are activated and forced into the hydrophobic nanopores. Due to the large surface area of HNPs, substantial mechanical energy is converted into solid-liquid interfacial energy and finally mitigated as heat during liquid flow process. With 1 wt% addition of nanoporous particles, the volumetric energy mitigation capacity of the LN-hydrogel can increase by 300%. Such hydrogel system provides a new paradigm for the design of energy dissipative hydrogels and holds great promise to tissue engineering and regenerative medicine applications.

1. Introduction

Cartilage damage and associated arthritis cause tremendous health and economic burdens to more than 21% of adults in the United States [1–3]. As innately lacking of energy mitigation capability of natural articular cartilage, daily activities impose substantial hydrostatic pressure on joints [4,5], and eventually lead to loss of joint motion, deformity, apoptosis, and inflammation [6–9]. To repair the defective articular cartilage, advanced biomaterials are in great demand. Due to extraordinary biocompatibility, high water content, and large porosity, synthetic hydrogels are appealing biomaterials for cartilage tissue regenerations [10–13]. However, existing hydrogels and their composites only dissipate energy under uniaxial loading [14–16] not hydrostatic pressure, the real loading condition of articular cartilage. Under hydrostatic loading conditions, hydrogels are usually considered as incompressible [17]. In addition, for long-term stability of repaired cartilage, fracture under hydrostatic pressure is destructive and an inappropriate energy mitigation mechanism. To the best of our knowledge, there is no report on energy mitigation mechanism of hydrogels under hydrostatic pressure.

The recent developed liquid nanofoam (LN) system, a highly compressible fluid system, has shown high energy mitigation capacity [18–20]. The energy mitigation mechanism is based on pressurized liquid flow in hydrophobic nanopores. In a typical LN system, hydrophobic nanoporous particles (HNPs) are suspended in a non-wettable liquid. Due to the capillary effect, liquid molecules are initially blocked at the hydrophobic nanopore entrance. When an applied external pressure is sufficiently high, the capillary effect is overcome and liquid molecules are forced into nanopores. Such process is referred to as liquid infiltration process, which mitigates large amount of mechanical energy into heat [18]. Instead of devastating the hollow structure, the efficient energy mitigation mechanism of LN is based on filling the nanopores by liquid molecules at pre-determined pressure [21]. In addition, the energy mitigation mechanism of the LN system is self-recoverable [22,23], which is vital for the development of cartilage substituting hydrogels.

By incorporating HNPs into hydrogel network, the liquid infiltration mechanism has the potential to functionalize the large amount of water confined in the hydrogel polymer network for energy mitigation under hydrostatic pressure. Please note that such energy mitigation mechanism is dominated by the liquid-nanopore interaction. Therefore, well-designed and elaborated preparation methods for strong polymer network structures are favorable but not necessary. For biomedical applications, good biocompatibility of HNPs is essential, which has been demonstrated in literature [24,25]. In current study, a single-network hydrogel impregnated with HNPs, denoted by LN-hydrogel, has been prepared and characterized under hydrostatic compression tests.

* Corresponding author.
E-mail address: wylu@egr.msu.edu (W. Lu).

https://doi.org/10.1016/j.coco.2020.05.003
Received 2 April 2020; Received in revised form 6 May 2020; Accepted 7 May 2020
Available online 16 May 2020
2452-2139/© 2020 Elsevier Ltd. All rights reserved.

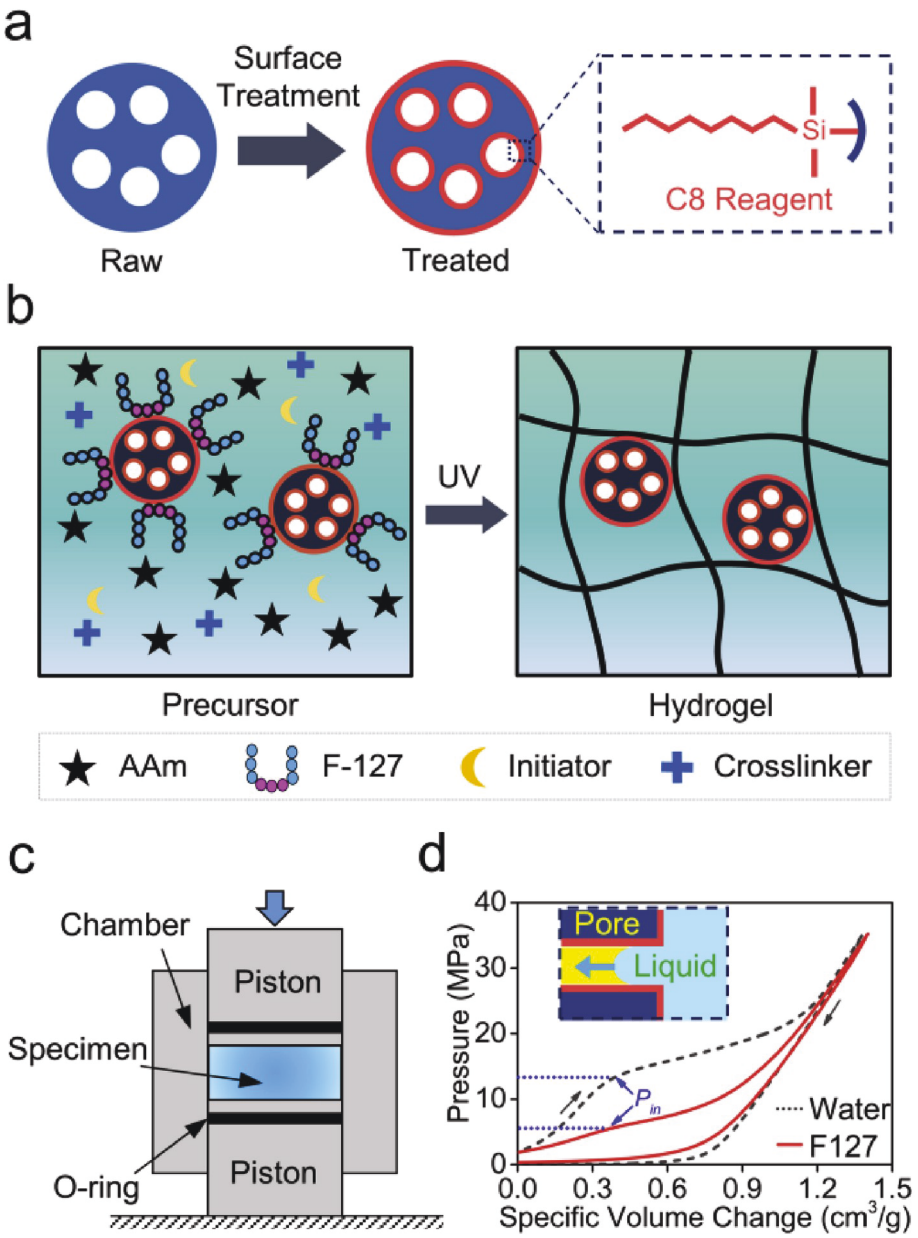

Fig. 1. (a) Schematic of hydrophobic surface treatment for HNPs. (b) Schematic of one-pot free-radical synthesis of LN-hydrogel synthesis. (c) The experimental setup for hydrostatic compression tests on LNs and LN-hydrogels. (d) Typical liquid infiltration mechanism and the constitutive mechanical behavior of different LNs.

2. Experimental procedure

To synthesize the LN-hydrogel, HNPs were prepared through surface modification. As shown in Fig. 1a, chloro(dimethyl)octylsilane (C8) was used as surface modification agent to graft a thin layer of silyl groups onto nanoporous silica gel spheres (SP120), as reported in our previous work [18]. The average pore size and particle size of the obtained HNPs (C8-SP120) were 120 Å and 10 μm, respectively. Then, C8-SP120 particles were mixed with polyacrylamide (PAM) aqueous precursor. To improve and stabilize the dispersion of C8-SP120, surfactant Pluronic® F127 was added into the aqueous mixture. After stirring for 1 h, the homogenized mixture was polymerized through the one-pot free-radical method (Fig. 1b). The resulted LN-hydrogels were fully swollen in deionized (DI) water before tests. Neat polyacrylamide (PAM) hydrogels were prepared by the same method and used as reference sample. The preparation procedure and characterization methods are detailed in Supplementary Information.

3. Results and discussion

Fig. 1c depicts a lab-customized quasi-static compression chamber, designed to characterize the liquid infiltration behavior of LNs. Two movable stainless-steel pistons are employed to seal LN specimens. The representative constitutive mechanical behavior of C8-SP120 in DI water and F127 aqueous solution are shown in Fig. 1d. For both LN systems, the initial elastic part of the loading curve is associated with the hydrostatic pressure build-up in the liquid phase, as the hydrophobic nanopore surface of C8-SP120 inhibits the liquid infiltration. For DI water-based LN, when the applied external pressure increases to 13 MPa, the slope of the loading curve suddenly decreases, indicating that the capillary effect at the hydrophobic liquid-nanopore interface has been overcome and liquid molecules are driven into the hydrophobic nanopores [20]. This critical pressure point is defined as the infiltration pressure (P_{in}). Following the classic Young-Laplace equation, $P_{in} = 2\gamma/r$, where γ is the effective solid-liquid interfacial tension and r is the effective radius of the nanopore [18]. The value of P_{in} is determined as

Table 1
Effective solid-liquid surface tension of C8-SP120-based liquid nanofoams containing different liquid phases.

Liquid Phase	P_{in}	γ
Water	13 MPa	39 mN/m
F127 solution	6 MPa	18 mN/m

the pressure at which the slope of the initial elastic loading curve reduces by 50%. Thereafter, a pressure plateau associated with the liquid infiltration process is observed. Due to the nanopore size distribution, liquid molecules start to fill larger nanopores and require additional pressure to enter smaller nanopores with the progress of liquid infiltration [19]. Therefore, the pressure plateau is not perfectly flat. The total width of the pressure plateau (ΔV_{sp}) is 0.8 cm^3/g, which is equivalent to the specific nanopore volume of C8-SP120. When the applied hydrostatic pressure reaches 24 MPa, all the nanopores are filled with water molecules and the LN becomes elastic again. The ending point of the infiltration plateau is defined at which the slope of the infiltration plateau increases by 50%. Upon unloading, the pressure drops drastically, resulting in a highly hysteretic behavior of the LN.

With the additional F127, the liquid infiltration behavior is similar to that of the DI water-based LN system. However, P_{in} and ΔV_{sp} are reduced by 52% and 9%, respectively. The F127 is a type of amphiphilic polyethylene oxide-polypropylene oxide-polyethylene oxide (PEO-PPO-PEO) triblock copolymer [26]. On one hand, the dispersion of the hydrophobic C8-SP120 spheres in the aqueous mixture is promoted by the hydrophobic interaction between the PPO block of F127 and the octyl end groups attached to the outer surface of C8-SP120 [27]. On the other hand, the hydrophilic PEO blocks of F127 reduce the surface tension of the liquid phase [28]. Therefore, the effective solid-liquid surface tension, which is the combined surface tension of the nanopore wall and the liquid phase in the nano-environment decreases and the P_{in} of the LN decreases from 13 MPa to 6 MPa. By following the classic Young-Laplace

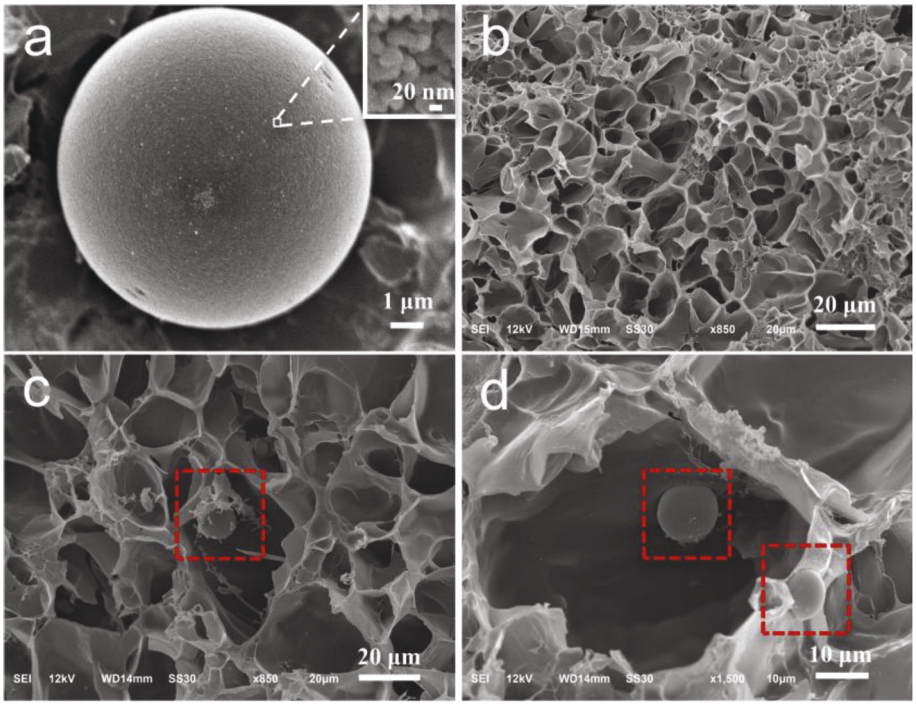

Fig. 2. SEM images of (a) C8-SP120 nanoporous sphere with a 10 μm diameter and open nanoporous network; (b–d) freeze-dried porous polymer network: (b) neat PAM hydrogel, (c) LN-hydrogel containing 2 wt% C8-SP120, and (d) LN-hydrogel containing 5 wt% C8-SP120.

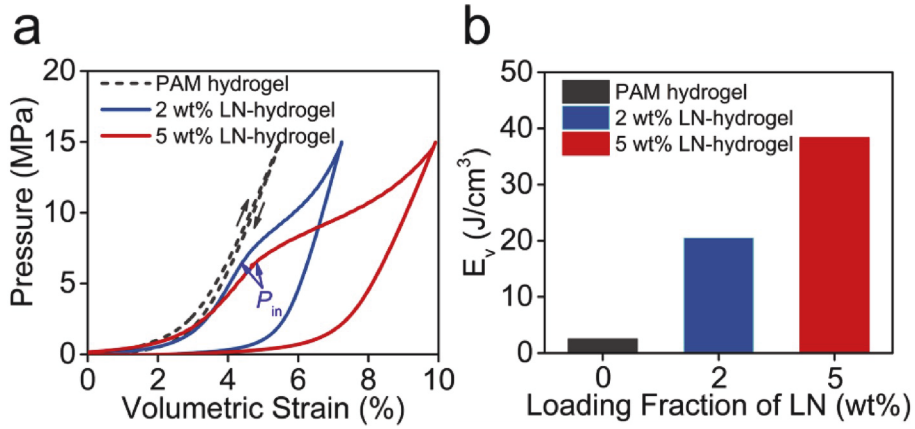

Fig. 3. (a) Constitutive mechanical behavior of LN-hydrogels under hydrostatic compression. (b) The energy mitigation capacity (E_v) of the LN-hydrogels with different loading.

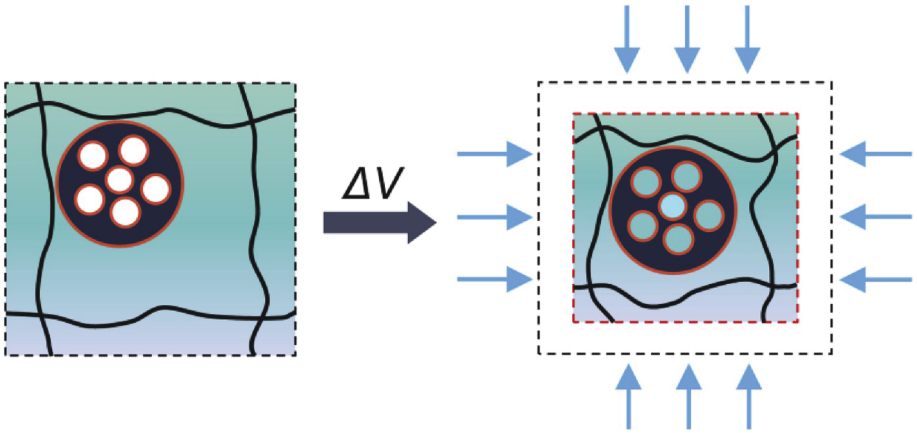

Fig. 4. Schematic of liquid infiltration process in PAM hydrogel network functionalized by surface-modified nanoporous particles.

equation, the effective solid-liquid surface tension is calculated and listed in Table 1. The ΔV_{sp} reduction from 0.80 to 0.73 cm^3/g is attributed to the larger micelle size of F127 in aqueous solution (~6 nm) [29]. This is much larger than the van der Waals diameter of water molecules (0.28 nm) [30], which limits the accessibility of the F127 solution to the hydrophobic nanopore surface.

As shown in Fig. 2a, the open nanoporous network of C8-SP120, which is essential for the liquid infiltration process, is observed under scanning electronic microscope (SEM). The polymer networks of neat PAM and LN-hydrogels are shown in Fig. 2b–d. Freeze-drying method is adopted to remove the confined water and preserve the porous structures of the different polymer networks. The porous structure of neat PAM hydrogels has pore diameters in the range of 5–20 μm. After the introduction of C8-SP120, the porous structure of LN-hydrogel is slightly changed. Most of the pores in the polymeric network still have a diameter in the range of 5–20 μm, while the pores containing C8-SP120 spheres possess larger diameter (~40 μm). This is attributed to the hydrophobic nature of C8-SP120 spheres. The hydrophilic acrylamide monomers are repelled away from C8-SP120 sphere during the polymerization process [31,32]. When the resulted polymer pockets are fully swollen by water, together with the encapsulated C8-SP120, local LN systems are formed in the LN-hydrogels. With increase loading fraction of C8-SP120, both the number of polymeric pockets containing C8-SP120 as well as the number of C8-SP120 spheres in a single polymeric pocket increase (Fig. 2d).

In order to evaluate the energy mitigation capacity of LN-hydrogels, the mechanical behavior of LN-hydrogel under hydrostatic pressure has been characterized. As shown in Fig. 3a, the neat PAM hydrogel undergoes pure elastic deformation and recovery. Please note that the initial concave section of the experiment is caused by system compliance of the mechanical tester. Since the hydrogel is fully swollen in water, the PAM network is nearly incompressible with a total volumetric strain smaller than 5%. When the external pressure is removed, the deformation is completely recovered. Therefore, the PAM hydrogel has negligible energy mitigation performance.

In contrast, the LN-hydrogels exhibit non-linear and highly hysteretic behavior. Once the applied hydrostatic pressure reaches 6.5 MPa, a pressure plateau similar to that of the liquid infiltration extends the deformability of the system (Fig. 3a). The initiation pressure of the plateau is close but slightly higher than the P_{in} of the F127 solution-based LN system, which is due to the affinity between the polymer chain and the confined liquid [33]. In addition, the width of the pressure plateau is linearly proportional to the loading fraction of C8-SP120 spheres in the LN-hydrogels. The specific volume change of the LN-hydrogels associated with the pressure plateau is around 0.70 cm^3/g, which is slightly smaller than the accessible pore volume of the F127 aqueous solution-based LN. These results demonstrate that the liquid infiltration process has been successfully activated, and thus significantly enhances the volumetric energy mitigation capacity (E_v) of the LN-hydrogels (Fig. 3b). With each 1 wt% additive C8-SP120, E_v is improved by 300%.

Please note, the energy mitigation mechanism is based on the non-destructive liquid motion into the nanopores, the LN-hydrogels have the potential to be further developed into repetitive energy absorbers [22,23]. In addition, the liquid infiltration mechanism is independent from the strain rate as reported in the previous study [19]. Although the polymeric network of the hydrogel is viscoelastic and strain-rate sensitive, the polymeric network only contributes ~10 wt% of the LN-hydrogel. Therefore, the dynamic behavior of the LN-hydrogel under hydrostatic loading condition is dominated by the liquid infiltration mechanism and anticipated to be strain-rate insensitive.

The detailed energy mitigation mechanism of the LN-hydrogel is illustrated in Fig. 4. The well-dispersed HNPs are surrounded by large amount of water to form local LN systems in the polymeric pocket. Once an applied external hydrostatic pressure reaches P_{in} of the encapsulated LN, the liquid infiltration process is activated inside the polymeric network. Correspondingly, the LN-hydrogel system has an enhanced volume reduction and mitigates large amount of mechanical energy. The polymer chains are relaxed during the liquid infiltration process, which is beneficial to preventing fracture. The embedded HNPs functionalize the major component of hydrogel systems, i.e. the confined liquid with up to 90 wt% in the material, for energy mitigation.

4. Conclusions

A hydrogel system that is capable of mitigating energy under hydrostatic compression has been developed by the incorporation of HNPs into PAM hydrogel network. Compare to the neat hydrogel, which has negligible energy mitigation capacity, the LN-hydrogels exhibit much enhanced energy mitigation capacity under hydrostatic compression. Such enhancement originates from the liquid infiltration energy mitigation mechanism of encapsulated HNPs in the polymeric network. In such way, the ultrahigh amount of water confined in hydrogels is functionalized by the HNPs for energy mitigation. This new energy mitigation mechanism holds great promise to improve the mechanical properties and durability of the next generation biomaterials for tissue regeneration.

Declaration of competing interest

The authors declare that they have no known competing financial interests or personal relationships that could have appeared to influence the work reported in this paper.

CRediT authorship contribution statement

Chi Zhan: Writing - original draft, Validation, Formal analysis, Investigation. **Mingzhe Li:** Methodology, Investigation, Writing - review & editing. **Weiyi Lu:** Conceptualization, Data curation, Writing - review & editing, Supervision, Funding acquisition, Project administration.

Acknowledgements

The authors are grateful for the financial support from the National Science Foundation (CBET-1803695).

Appendix A. Supplementary data

Supplementary data related to this article can be found at https://doi.org/10.1016/j.coco.2020.05.003.

References

[1] E. Yelin, M. Cisternas, A. Foreman, D. Pasta, L. Murphy, C. Helmick, National and state medical expenditures and lost earnings attributable to arthritis and other rheumatic conditions–United States, 2003, Morb. Mortal. Wkly. Rep. 56 (1) (2007) 4–7.
[2] D.L. Blackwell, J.W. Lucas, T.C. Clarke, Summary health statistics for US adults: national health interview survey, Vital Health Stat 10 (260) (2014) 1–161, 2012.
[3] K.E. Barbour, C.G. Helmick, M. Boring, T.J. Brady, Vital signs: prevalence of doctor-diagnosed arthritis and arthritis-attributable activity limitation—United States, 2013–2015, Morb. Mortal. Wkly. Rep. 66 (9) (2017) 246.
[4] R.L. Smith, M. Trindade, J. Shida, G. Kajiyama, T. Vu, Time-dependent effects of intermittent hydrostatic pressure on articular c on rocyte type II collagen and aggrecan mRNA expression, J. Rehabil. Res. Dev. 37 (2000) 153–161.
[5] S. Mizuno, R. Ogawa, Using changes in hydrostatic and osmotic pressure to manipulate metabolic function in chondrocytes, Am. J. Physiol. Cell Physiol. 300 (6) (2011) C1234–C1245.
[6] E.L. Radin, H.G. Parker, J.W. Pugh, R.S. Steinberg, I.L. Paul, R.M. Rose, Response of joints to impact loading—III: relationship between trabecular microfractures and cartilage degeneration, J. Biomech. 6 (1) (1973) 51–57.
[7] J.A. Buckwalter, Mechanical injuries of articular cartilage, Iowa Orthop. J. 12 (1992) 50.
[8] R.L. Smith, S. Rusk, B. Ellison, P. Wessells, K. Tsuchiya, D. Carter, W. Caler, L. Sandell, D. Schurman, In vitro stimulation of articular chondrocyte mRNA and extracellular matrix synthesis by hydrostatic pressure, J. Orthop. Res. 14 (1) (1996) 53–60.
[9] K. Montagne, Y. Onuma, Y. Ito, Y. Aiki, K.S. Furukawa, T. Ushida, High hydrostatic pressure induces pro-osteoarthritic changes in cartilage precursor cells: a transcriptome analysis, PloS One 12 (8) (2017).
[10] J. Kisiday, M. Jin, B. Kurz, H. Hung, C. Semino, S. Zhang, A. Grodzinsky, Self-assembling peptide hydrogel fosters chondrocyte extracellular matrix production and cell division: implications for cartilage tissue repair, Proc. Natl. Acad. Sci. U. S. A 99 (15) (2002) 9996–10001.
[11] H. Bodugoz-Senturk, C.E. Macias, J.H. Kung, O.K. Muratoglu, Poly (vinyl alcohol)–acrylamide hydrogels as load-bearing cartilage substitute, Biomaterials 30 (4) (2009) 589–596.
[12] K.L. Spiller, S.A. Maher, A.M. Lowman, Hydrogels for the repair of articular cartilage defects, Tissue Eng. B Rev. 17 (4) (2011) 281–299.
[13] I.L. Kim, R.L. Mauck, J.A. Burdick, Hydrogel design for cartilage tissue engineering: a case study with hyaluronic acid, Biomaterials 32 (34) (2011) 8771–8782.
[14] J.P. Gong, Y. Katsuyama, T. Kurokawa, Y. Osada, Double-network hydrogels with extremely high mechanical strength, Adv. Mater. 15 (14) (2003) 1155–1158.
[15] X. Zhao, Designing toughness and strength for soft materials, Proc. Natl. Acad. Sci. U. S. A 114 (31) (2017) 8138–8140.
[16] Z. Wang, C. Xiang, X. Yao, P. Le Floch, J. Mendez, Z. Suo, Stretchable materials of high toughness and low hysteresis, Proc. Natl. Acad. Sci. U. S. A 116 (13) (2019) 5967–5972.
[17] T. Baumberger, C. Caroli, D. Martina, Solvent control of crack dynamics in a reversible hydrogel, Nat. Mater. 5 (7) (2006) 552–555.
[18] M. Li, W. Lu, Liquid marble: a novel liquid nanofoam structure for energy absorption, AIP Adv. 7 (5) (2017), 055312.
[19] M. Li, W. Lu, Adaptive liquid flow behavior in 3D nanopores, Phys. Chem. Chem. Phys. 19 (26) (2017) 17167–17172.
[20] Y. Zhang, M. Li, Y. Gao, B. Xu, W. Lu, Compressing liquid nanofoam systems: liquid infiltration or nanopore deformation? Nanoscale 10 (39) (2018) 18444–18450.
[21] D. Hu, H. Jiang, K. Meng, J. Xu, W. Lu, The impact mitigation of a heterojunction nanotube–water system: behavior and mechanism, Phys. Chem. Chem. Phys. 18 (10) (2016) 7395–7403.
[22] M. Li, L. Xu, W. Lu, Nanopore size effect on critical infiltration depth of liquid nanofoam as a reusable energy absorber, J. Appl. Phys. 125 (4) (2019), 044303.
[23] L. Xu, M. Li, W. Lu, Effect of electrolytes on gas oversolubility and liquid outflow from hydrophobic nanochannels, Langmuir 35 (45) (2019) 14505–14510.
[24] M. Zhao, C. Deng, X. Zhang, Synthesis of C8-functionalized magnetic graphene with a polydopamine coating for the enrichment of low-abundance peptides, ChemPlusChem 79 (3) (2014) 359–365.
[25] H. Jaganathan, B. Godin, Biocompatibility assessment of Si-based nano-and micro-particles, Adv. Drug Deliv. Rev. 64 (15) (2012) 1800–1819.
[26] K. Mortensen, W. Batsberg, S. Hvidt, Effects of PEO− PPO diblock impurities on the cubic structure of aqueous PEO− PPO− PEO pluronics micelles: fcc and bcc ordered structures in F127, Macromolecules 41 (5) (2008) 1720–1727.
[27] A. Yildirim, G.B. Demirel, R. Erdem, B. Senturk, T. Tekinay, M. Bayindir, Pluronic polymer capped biocompatible mesoporous silica nanocarriers, Chem. Commun. 49 (84) (2013) 9782–9784.
[28] G.-E. Yu, Y. Deng, S. Dalton, Q.-G. Wang, D. Attwood, C. Price, C. Booth, Micellisation and gelation of triblock copoly (oxyethylene/oxypropylene/oxyethylene), F127, J. Chem. Soc., Faraday Trans. 88 (17) (1992) 2537–2544.
[29] Y.-M. Lam, N. Grigorieff, G. Goldbeck-Wood, Direct visualisation of micelles of Pluronic block copolymers in aqueous solution by cryo-TEM, Phys. Chem. Chem. Phys. 1 (14) (1999) 3331–3334.
[30] F. Franks, Water: a Matrix of Life, Royal Society of Chemistry, 2007.
[31] R.A. Gemeinhart, H. Park, K. Park, Pore structure of superporous hydrogels, Polym. Adv. Technol. 11 (8-12) (2000) 617–625.
[32] X.z. Zhang, C.c. Chu, R.x. Zhuo, Using hydrophobic additive as pore-forming agent to prepare macroporous PNIPAAm hydrogels, J. Polym. Sci., Part A: Polym. Chem. 43 (22) (2005) 5490–5497.
[33] Y. Tamai, H. Tanaka, K. Nakanishi, Molecular dynamics study of polymer− water interaction in hydrogels. 2. Hydrogen-bond dynamics, Macromolecules 29 (21) (1996) 6761–6769.